Biosensors and Bioelectronics 70 (2015) 404–410

Contents lists available at ScienceDirect

Biosensors and Bioelectronics

journal homepage: www.elsevier.com/locate/bios

Enzyme-guided plasmonic biosensor based on dual-functional nanohybrid for sensitive detection of thrombin

Jing Yan, Lida Wang, Longhua Tang, Lei Lin, Yang Liu, Jinghong Li *

Department of Chemistry, Beijing Key Laboratory for Analytical Methods and Instrumentation, Tsinghua University, Beijing 100084, China

ARTICLE INFO

Article history:
Received 4 January 2015
Received in revised form
5 March 2015
Accepted 9 March 2015
Available online 16 March 2015

Keywords:
Localized surface plasmon resonance (LSPR)
Gold nanoparticle
Dual functional nanomaterial
Nanohybrid
Thrombin
Enzyme
Plasmonic biosensor

ABSTRACT

Rapid and sensitive methodologies for the detection of protein are in urgent requirement for clinic diagnostics. Localized surface plasmon resonance (LSPR) of metal nanostructures has the potential to circumvent this problem due to its sensitive optical properties and strong electromagnetic near-field enhancements. In this work, an enzyme mediated plasmonic biosensor on the basis of a dual-functional nanohybrid was developed for the detection of thrombin. By utilizing LSPR-responsive nanohybrid and anaptamer-enzyme conjugated reporting probe, the sensing platform brings enhanced signal, stability as well as simplicity. Enzymatic reaction catalyzed the reduction of Au^{3+} to Au° *in situ*, further leading to the rapid crystal growth of gold nanoparticles (AuNPs). The LSPR absorbance band and color changed company with the nanoparticle generation, which can be real-time monitoring by UV–visible spectrophotometer and naked eye. Nanohybrid constructed by gold and magnetic nanoparticles acts as a dual functional plasmonic unit, which not only plays the role of signal production, but also endows the sensor with the function of magnetic separation. Simultaneously, the introduction of enzyme effectively regulates the programming crystal growth of AuNPs. In addition, enzyme also serves as signal amplifier owing to its high catalysis efficiency. The response of the plasmonic sensor varies linearly with the logarithmic thrombin concentration up to 10 nM with a limit of detection of 200 pM. The as-proposed strategy shows good analytical performance for thrombin determination. This simple, disposable method is promising in developing universal platforms for protein monitoring, drug discovery and point-of-care diagnostics.

1. Introduction

Development of sensitive and rapid methods for detection of proteins is in urgent requirement for medical diagnostics and therapeutics. (Jans and Huo, 2012; Song et al., 2010; Whitcombe et al., 2011; Deng et al., 2014; Wang et al., 2014) Various strategies, including electrochemical analyses, (Nie et al., 2009) enzyme-linked immunosorbent assay (ELISA), (Fredriksson et al., 2002) PAGE, (Vallejo-Illarramendi et al., 2013) have been demonstrated for detecting different kinds of proteins. Although these well established methods have been broadly used, they are time-consuming, complex, and usually rely on expensive and sophisticated instrument. Therefore, it is still of great challenge to develop protein sensors for rapid and simple point-of-care (POC) diagnostics that can be used by untrained personnel. (Liu et al., 2013; Luppa et al., 2011)

Localized surface plasmonresonance (LSPR) has emerged as an increasingly popular tool for protein analysis with high sensitivity due to its optical properties and strong electromagnetic near-field enhancements.(Haes et al., 2004; McFarland and Van Duyne, 2003; Zhao et al., 2009) LSPR of gold nanoparticle comes from light excited collective surface plasmon oscillations on the surface of metallic nanoparticles. It demonstrates the characteristics of sharp absorption peak in the visible wavelengths range at the macro level. The LSPR properties greatly affect by size and interparticle distance of the metal nanoparticles, which is reflected in color change and absorption peak shift. (Mayer and Hafner, 2011) Pioneer works have shown its advantages in constructing diverse biosensor for disease diagnostics. (Sepúlveda et al., 2009) However, these assays are usually lack of efficient separation method, which is a big limitation for practical POC diagnostic in homogeneous solution. Fe_3O_4 magnetic nanoparticle has been widely applied in isolation area owing to its excellent superaramagnatic ability. Additionally, high surface area and good biocompability make it feasible to hybrid with other nanomaterials and biomolecules. (Boterashvili et al., 2012; Chemla et al., 2000; Goon et al., 2009; Jiang et al., 2008; Perez et al., 2003; Rogstad et al., 2013; Tong et al., 2012) Nanocomposites made of gold and Fe_3O_4

* Corresponding author.
E-mail address: jhli@mail.tsinghua.edu.cn (J. Li).

http://dx.doi.org/10.1016/j.bios.2015.03.024
0956-5663/

nanoparticlenot only provide aneffective solution to the sophisticated operation of traditional plasmonic biosensors, but also extend its application in point-of-care diagnostics.

As we all know, enzyme acts as an efficient catalyst to tailor the shape and size of nanostructure. It guides programming crystal growth of AuNPs and tunes its chemicophysieal property consequently. (de La Rica and Stevens, 2012; Liz-Marzan, 2006; Rodríguez-Lorenzo et al., 2012; Willner et al., 2006) Thus, enzyme-AuNPs conjugates can provide biocatalytic systems that serve as amplifying units in practical applications. Pioneer works which take advantage of these properties for biosynthsis have been well established. (Ahmad et al., 2002; Rangnekar et al., 2007) Combining the high efficient catalysis property of enzyme with the sensitive LSPR-response character of AuNPs will offer a sensitive sensing strategy. However, the development of biodetection derived from this concept is still on the early stage.

Here we constructed a dual functional AuNPs/Fe_3O_4 nanohybrid, upon which a novelplasmonic sensor for protein detection was built for the first time. On this platform, the signal probe modified with glucose oxidase can *in situ* generate H_2O_2 to initiate the crystal growth and produce a colorimetric readout signal. Aptameris chosen as the recognition element owing to its high binding affinity and chemical stability compared with its antibody counterparts. (Farokhzad et al., 2006; Huizenga and Szostak, 1995; Macaya et al., 1993; Pavlov et al., 2004) Aptamer I was used to capture target analyte specifically, which also allows easy removal of excess protein and other unbound objects with magnetic separation. Aptamer II, which is connected to glucose oxidase (Aptamer II/GOx), binds to the captured protein. Subsequently, nanoparticle growth reaction is performed where the product of H_2O_2 can reduce the Au^{3+} ions in the solution to Au°. The depositon of Au° on the AuNPs surface can enlarge the size of the nanoparticle, which significantly alters the LSPR property. As a result, a significant plasmonic absorption peak variation emerged, along with the color change of the mixture, which can be recognized by naked eye and measured through spectrophotometer. Here, we used thrombin as a model target, as it is essential in regulation of tumor growth, angiogenesis and metastasis. (Chang et al., 2010; Cho et al., 2008; He et al., 2007; Pavlov et al., 2004) Taking advantage of enzyme assisted AuNPs crystal growth and magnetic separation, simple, sensitive and selective sensing platform can be successfully realized in homogeneous solution.

2. Experimental section

2.1. Reagents

Thrombin (from human plasma) was purchased from Sigma. The DNA sequences were obtained from Shanghai Sangon Biological Engineering Technology & Services Co., Ltd. DNA sequence of thrombin aptamer was listed as follows: Aptamer I (P1): 5′-SH-(CH_2)-TTT AGT CCG TGG TAG GGC AGG TTG GGG TGA CT-3′; Aptamer II (P2), 5′-NH_2-(CH_2)-GGT TGG TGT GGT TGG-3′. Glucose oxidase, bovine serum albumin (BSA), immunoglobulin G (IgG) and hemoglobin were bought from Beijing DingGuo Biotech. Co., Ltd. $HAuCl_4$ was bought from Alfa Aesar (Tianjing, China). Other regents of analytical grade were purchased from Beijing Chemical Co. (Beijing, China). Deionized water was used for all solutions preparation.

2.2. Synthesis of AuNPs/Fe_3O_4 nanohybrid

The gold colloid and the Fe_3O_4 nanoparticles were synthesized according to previous reports. (Brown et al., 2000; Hui et al., 2008; Jana et al., 2001) As for the preparation of the nanohybrid, 100 mL of 0.6 mg/mL Fe_3O_4 nanoparticle solution was first sonicated for 15 min, following by slow addition of 2.5 mL of 2.5 mg/mL (polyethylenimine) PEI solution (pH 10.0). Magnetic separation method was used to remove redundant PEI for three times. Afterwards, 45 mL gold colloid solution was added to the PEI coated Fe_3O_4 solution. The resulting solution was washed with deionized water for three times to remove the redundant gold colloids and stored in 10 mg/mL BSA at room temperature for future use.

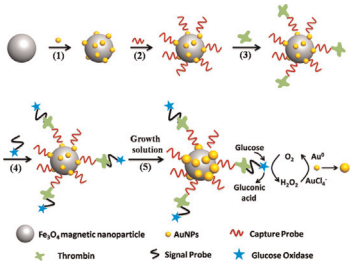

Scheme 1.
Schematic Illustration of AuNPs/Fe_3O_4 Nanohybrid Based Plasmonic Sensor and the Mechanism of Thrombin Detection. (1) AuNPs are loaded onto Fe_3O_4 magnetic nanoparticles surface to obtain the dual functional composite nanomaterial; (2) Capture probe (thrombin aptamer I) is bounded to the nanohybrid via covalent bond; Owing to the double aptamer recognition mechanism, in the presence of thrombin (3) and aptamer II/glucose oxidase(4), a sandwiched structure was formed and (5) with the addition of "gold nanoparticle growth solution" ($HAuCl_4$ and glucose), crystal growth is initiated, resulting in size enlargement, absorption peak shift and color change.

2.3. DNA functionalization of AuNPs/Fe_3O_4 nanohybrid

Thiol-modified thrombin aptamer was attached onto AuNPs/Fe_3O_4 nanohybridin accordance with previous reported protocols. (Zhang et al., 2012) Briefly, 10 uL of 100 uM thiol-modified thrombin aptamerI stock solution was mixed with 1 mL above prepared AuNPs/Fe_3O_4 nanohybrid solution and incubated for 2 min. Afterwards, the sample was adjusted to acidity with 300 mM citrate · HCl buffer (pH 3.0). Concentrated NaCl was gradually added into the solution to increase the NaCl concentration to 300 mM with gentle shake. Extra AuNPs were removed through PBS washing and magnetic separation. The obtained DNA-functioned AuNPs/Fe_3O_4 nanohybrid was redispersed in 10 mg/mL (PBS) solution for future use.

2.4. Preparation of glucose oxidase modified thrombin aptamerII.

The glucose oxidase modified signal probe was prepared with the aid of glutaraldehyde, which isfrequently used as an amine-reactive cross linking reagent. (Hao et al., 1998; Thompson et al., 1991; Williams and Tjian, 1991) In general, 35 uL of 200 uM amine group-modified thrombin aptamer II stock solution was mixed with 35 uL of 400 uM glucose oxidase solution and stirred for 10 min. Freshly prepared glutaraldehyde solution (70 uL, 2 wt%) was put into the mixture and shaked on an oribital shaker for 1 min, followed by 30 min incubation at room temperature. After that, Tris–HCl buffer (10 uL, 50 mM, pH 7.0) was used to terminate the reaction. Unreacted glucose oxidase was removed by centrifugal ultrafiltration (Millipore, Amicon Ultra-2, molecular weight cutoff: 30 kDa) and redissolved in PBS solution.

2.5. Assembly of the plasmonic sensor

For the detection of the target, 100 uL thrombin aptamerI modified AuNPs/Fe_3O_4 nanohybrid prepared above was mixed with 100 uL PBS solution (10 mM PBS, 100 mM NaCl, pH 7.40) containing a certain amount of thrombin and incubated for 30 min. After careful wash and separation, the nanohybrid was

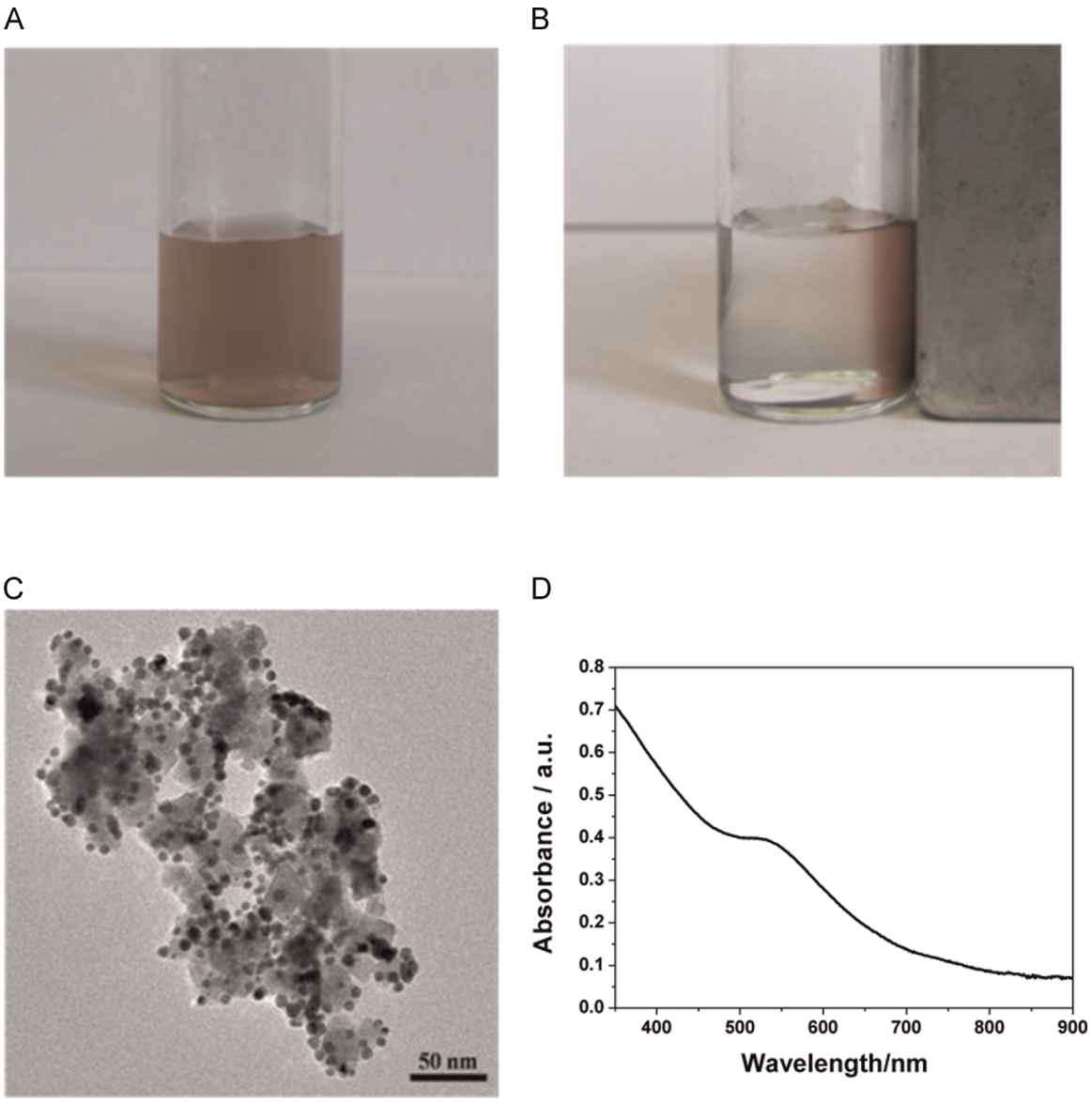

Fig. 1. Photographs of Fe_3O_4/AuNPs nanohybrid (A) and its behavior under the influence of a magnetic field (B). Highresolution TEM image (C) and UV-visible absorption spectra (D) of Fe_3O_4/AuNPs nanohybrid.

mixed with 2 uL GOx modified thrombin aptamerII at 37 °C for 20 min. Finally, the nanohybrid were separated with magnet and stored in PBS buffer for further usage.

2.6. The growth of the gold nanoparticle and the UV-visibleDetection

The crystal growth of gold nanoparticle was carried out in PBS buffer for 20 min (37 °C). To evaluate the crystal growth, "gold nanoparticles growth solution" (6 uL of 5 mM $HAuCl_4$ and 40 uL of 2 M glucose) and 100 uL AuNPs/ Fe_3O_4 nanohybrid solution obtained last step were put into 200 uL reaction buffer. The mixture was the incubated at 37 °C for 20 min in dark, followed by magnetic separation and washing with PBS buffer. UV-visible spectra detection was carried out on a UV-visible spectrophotometer at room temperture.

3. Results and discussion

3.1. Strategy for thrombin detection

The plasmonic strategy developed for the detection of thrombin is illustrated in Scheme 1. The formation of dual functional AuNPs/Fe_3O_4 nanohybrid was accomplished with a polycationic polymer (PEI). A thiol-modified thrombin specific aptamer which acts as a capture probe was attached on the surface of AuNPs/Fe_3O_4 nanohybrid by forming gold – sulfur bond covalently. Adequate aptamerI on the surface of the nanohybrid can further gurantee the following effective capture of the target thrombin owing to the high binding affinity between aptamerI and heparin-binding site of thrombin ($K_d \approx 0.5$ nM). A secondary thrombin aptamerIIbinding to the fibrinogen-binding site of thrombin ($K_d \approx 100$ nM), was conjugated with glucose oxidase, which played the role of binding and signal reporting probe. A sandwich type system was then obtained through the two aptamers target at different epitopes of one thrombin. With the presence of "gold nanoparticle growth solution", enzyme catalyzed the transformation of gold ions around the AuNPs into Au°, which subsequently changes the LSPR property of the nanohybrid. While, in the absence of thrombin, glucose oxidase on the signal probe failed to attach onto the nanohybrid surface and was quickly wiped away by efficient magnetic separation. Thus no obvious LSPR band shift was observed after the addition of thrombin. Therefore, the

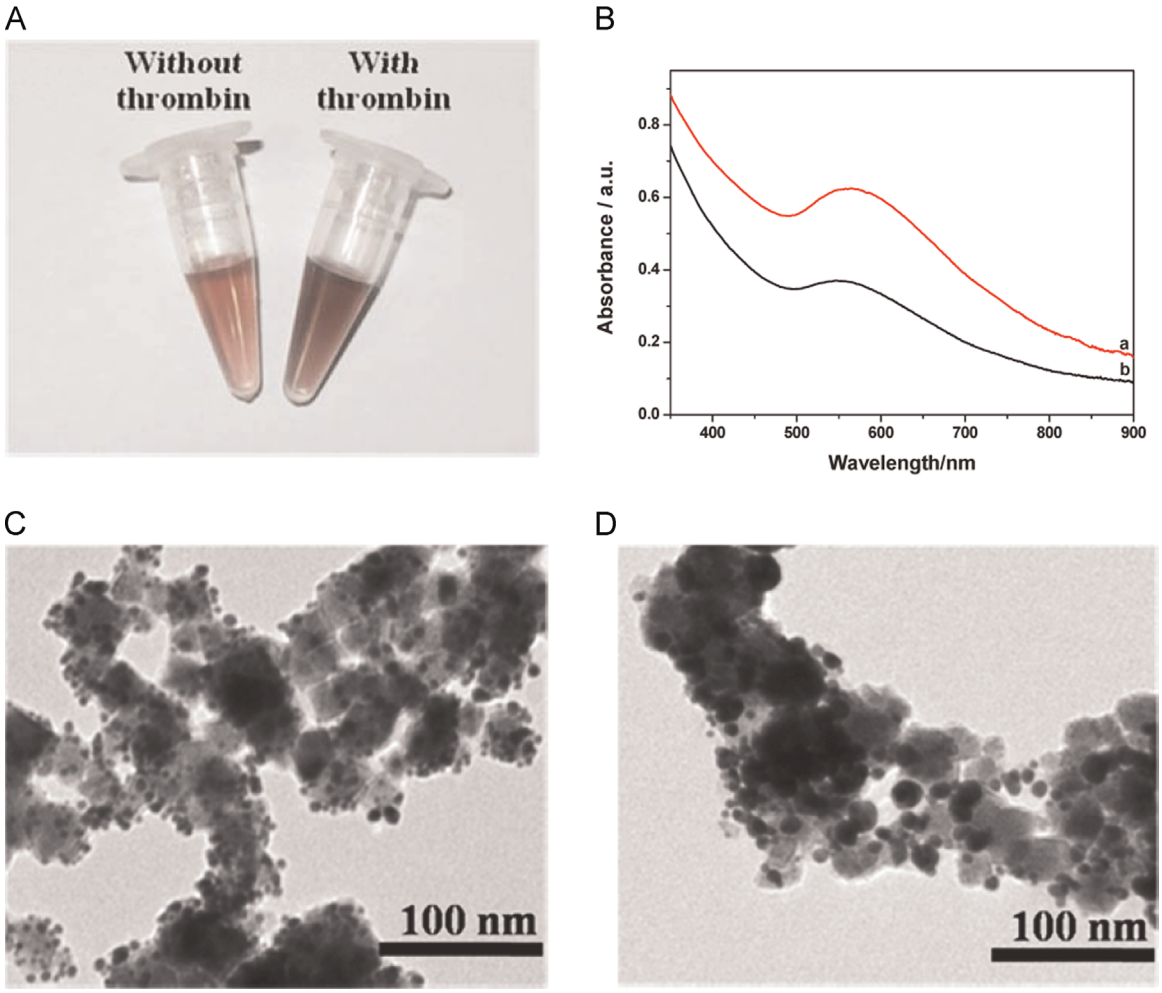

Fig. 2. (A) Photographs of the AuNPs/ Fe_3O_4 nanohybrid without (left) and with (right) thrombin addition; corresponding UV-visible absorption spectra is shown in (B): with (a) and without (b) thrombin. TEM images of the nanohybrid without (C) and with (D) thrombin. The concentrations of $HAuCl_4$, glucose and thrombin were 150 uM, 400 mM and 10 nM, respectively.

concentration of thrombin can be easily reflected by the UV-visible spectra alteration and color change.

3.2. *Characterization of the AuNPs/ Fe_3O_4 nanohybrid*

As shown in Fig. 1A, the color of the AuNPs/Fe_3O_4 nanohybrid was dark red. Meanwhile, the composite nanomaterials can be easily attracted by an external magnetic field (Fig. 1B), which shows its significant magnetic separation capacity in the plasmonic biosensor.The high resolution TEM image of the as prepared AuNPs/ Fe_3O_4 nanohybridis displayed in Fig. 1C. The diameter of the Fe_3O_4 nanoparticle was about 30 nm, which is much larger than the size of AuNPs. It is also the reason why one Fe_3O_4 particle could load several AuNPs to form the nanohybrid. The relatively large amount of AuNPs on the nanohybrid surface provides adequate active sites for the immobilization of capture probe. Fig. 1D shows the UV-visible absorption spectra of AuNPs/Fe_3O_4 nanohybrid. Before crystal growth, the LSPR band of the AuNPs/Fe_3O_4 composite nanomaterial appears at ~540 nm. A thiolated thrombin aptamer I was attached on the AuNPs via covalent reaction. The quantity of capture probe attached on the AuNPs/Fe_3O_4 composite nanomaterial was estimated to be 200-300 nM.

3.3. *Detection capability of the plasmonic biosensor*

Fig. 2 manifests the photograph, UV-visible absorption spectra and TEM characteration of the AuNPs/Fe_3O_4 nanohybrid after the coupled enzyme reaction with and without the addition of thrombin. Compared with none thrombin assay, the color of the AuNPs/Fe_3O_4 nanohybrid solution changed in the presence of thrombin, which can be obviously seen in Fig. 2A. Along with that, a LSPR band red-shift and absorbance increase can be detected by spectrophotometer (Fig. 2B). The fact is attributed to strong binding affinity between thrombin and the double aptamers and the high catalysis capacity of the enzyme. The phenomenon was further confirmed with transmission electron microscopy (TEM). As shown in Fig. 2C, without the existence of thrombin, the tiny gold nanoparticles on the edge of the Fe_3O_4 nanoparticle was estimated to be about 5–10 nm. When thrombin initiated the enzymatic reactions, a size enlargement of the gold nanoparticles can be clearly seen, as demonstrated in Fig. 2D, which is in consistent with the LSPR state. These results indicate that the as proposed strategy can ensure the thrombin detection in the future.

3.4. *Optimization of the experimental Conditions*

The concentration of $HAuCl_4$ affects the performance of the plasmonic biosensor in a close way. As can be seen in Fig. 3C, the UV-visible absorbance intensity increased with the concentration of $HAuCl_4$ and then reached its maximum at the $HAuCl_4$ concentration of 150 uM. Additional $HAuCl_4$ will not benefit the signal enlargement. On the other contrary, when the concentration of

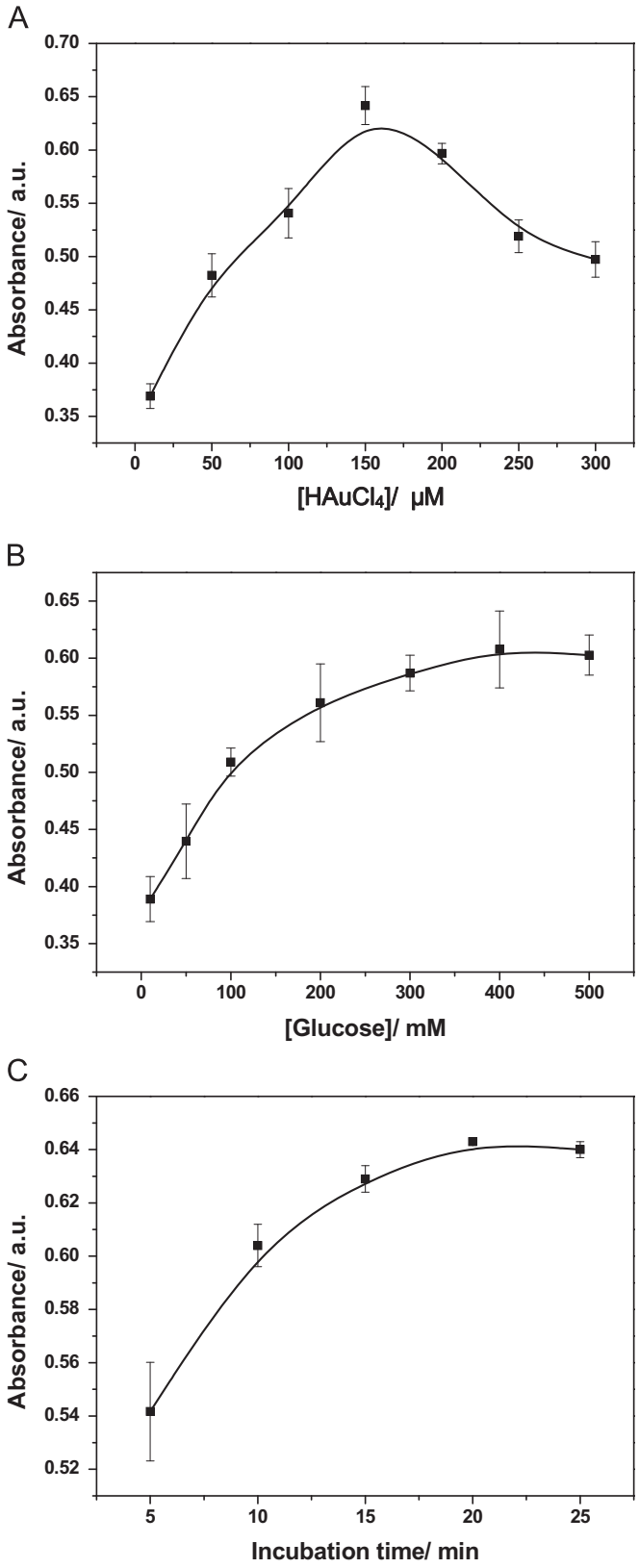

Fig. 3. (A) Optimization of $HAuCl_4$ concentration. The concentration glucose was 400 mM. (B) Optimization of glucose concentration. The concentration of $HAuCl_4$ was 150 μM. (C) Optimization of the reaction time. The concentrations of $HAuCl_4$ and glucose were 150 μM and 400 mM. For all the assays, the concentration of thrombin was 10 nM. The UV-visible absorption spectra peak intensity for analysis was obtained at 560 nm.

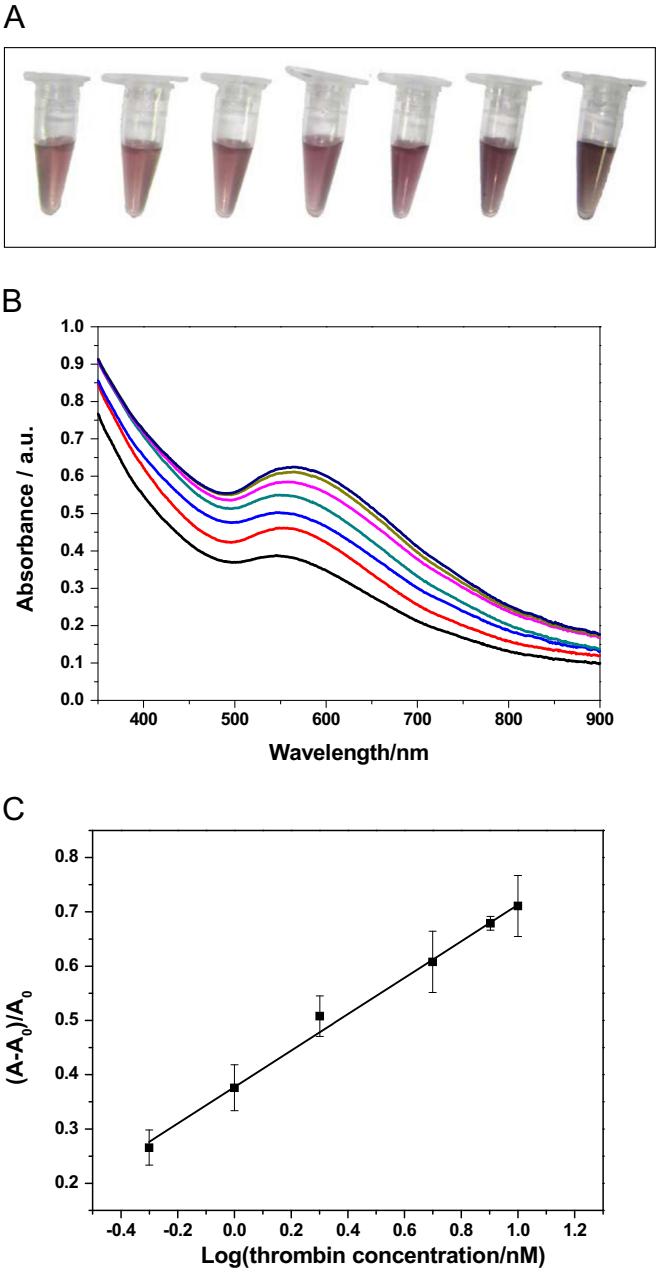

Fig. 4. (A) Photograph of AuNPs/ Fe_3O_4 nanohybrid after crystal growth with different concentrations of thrombin (from left to right: 0, 0.5, 1, 2, 5, 8 and 10 nM) in PBS buffer (pH 7.40). (B) Relative UV-visible absorption spectra changes of AuNPs/ Fe_3O_4 nanohybrid via thrombin concentrations (from bottom to up: 0, 0.5, 1, 2, 5, 8 and 10 nM). Relative absorption spectra changes are defined as $(A-A_0)/A_0$, where A_0 and A are absorption intensities without and with thrombin, respectively. The concentrations of $HAuCl_4$ and glucose were 150 uM and 400 mM respectively.

$HAuCl_4$ was higher than 150 uM, the absorbance in the region decreased again due to the strong acid property and the bright yellow color of $HAuCl_4$. Hence, the optimal concentration of $HAuCl_4$ was selected to be 150 uM.

As the growth of the AuNP shighly relies on the enzymatic reaction of glucose oxidase and its substrate, the concentration of glucose is also animportant parameter for the plasmonic biosensor. As indicated in Fig. 3A, a significant increase of the UV-visible absorbance intensity of the nanohybrid is observed with increasing the concentration of glucose in the "growth solution". It tended to reach a steady value after 400 mg/mL, indicating a tendency of saturated concentration for the enzymatic reaction.

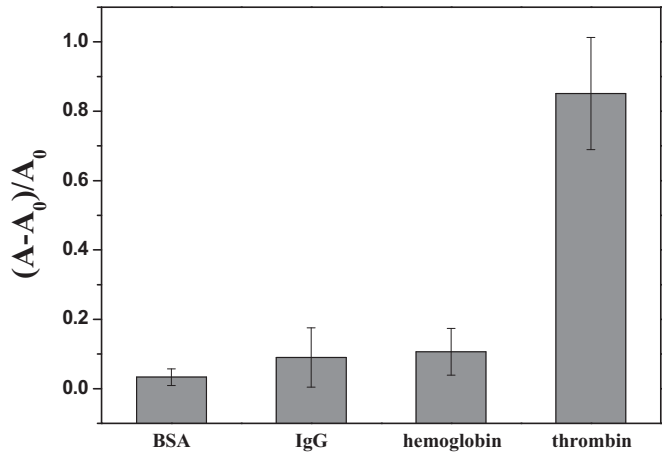

Fig. 5. Relative UV-visible absorption intensity of the plasmonic biosensor incubated with 1 uM BSA, IgG and hemoglobin in PBS; 10 nM thrombin in PBS, respectively. The concentrations of $HAuCl_4$ and glucose were 150 uM and 400 mM respectively. Wavelength: 560 nm.

Future more, the incubation time of the AuNPs/ Fe_3O_4 nanohybrid in the "growth solution" is another important factor for the sensitivity of the plasmonic biosensor. With increasing the incubation period up to 25 min, the UV-visible absorbance intensity of the AuNPs/ Fe_3O_4 hybrid gradually raised and finally arriveda plateau at 20 min (Fig. 3B). Thus, the optimized incubation time was 20 min.

3.5. Thrombin detection with plasmonic biosensor

According to the optimized reaction condition, the plasmonic biosensor was used for thrombin detection. Fig. 4 demonstrates the UV-visible absorbance signal variation of the biosensor in response of thrombin of different concentrations. The UV-visible absorbance peak (at 560 nm) intensities are proportional to the logarithmic value of the thrombin concentration from 500 pM to 10 nM. The linear regression equation is $R_{uv}=0.377+0.336\times \log C_{thrombin}$ (nM) with the correlation coffecient of $R^2=0.990$, where R_{uv} is the relative UV-visible absorbance intensity at 560 nm and $C_{thrombin}$ is the concentration of thrombin. The detection limit for thrombin was 200 pM in a total 100 uL volume. The results indicate that sensitive and accurate detection of thrombin can be achieved through dual functional nanohybrid based plasmonic biosensor.

3.6. Selectivity of the plasmonic biosensor

In our experiments, bovine serum albumin (BSA), immunoglobulin G (IgG) and hemoglobin were chosen to investigatethe specificity of the plasmonic biosensor. In a typical experiment, 1 uM BSA, human IgG and hemoglobin were incubated with capture probe modified AuNPs/Fe_3O_4 nanohybrid instead of thrombin, respectively. It is observed from Fig. 5 that UV-visible absorbance intensity of the AuNPs/Fe_3O_4 nanohybrid was relatively low for BSA, human IgG and hemoglobin. However, the UV-visible absorbance peak made a significant red-shift and the intensity increased greatly in the case of thrombin. The relative UV-visible absorbance intensity $(A-A_0)/A_0$ of the plasmonic biosensor in the presence of thrombin is 0.851, which is much higher than that of 0.033 for BSA, 0.090 for IgG and 0.107 for hemoglobin. The good selectivity of the plasmonic biosensor is mainly due to the high specificity of thrombin aptamer. These results manifest that thrombin can be detected with high selectivity.

4. Conclusion

In summary, a plasmonic biosensor for thrombin detection has been constructed using glucose oxidase guided crystal growth and the dual functional AuNPs/Fe_3O_4 nanohybrid platform. The efficient catalysis capacity of glucose oxidase and the sensitive LSPR property of AuNPs both contribute to the good analytical performance of the biosensor. In addition, the utilization of dual functional nanohybrid makes the detection procedure easy to perform, and avoids the complicated operation in target isolation and signal process. Simultaneously, the introduction of enzyme guides the programming crystal growth of AuNPs effectively. Furthermore, it also acts as signal amplifier due to its high catalysis efficiency. The colorimetric nature and its chemical stability benefit our sensor with low cost and simplicity, which makes it possible in point-of-care applications. The as-proposed strategy provides a linear range from 0.5 nM to 10 nM and a low detection limit of 0.5 nM for thrombin analysis with high selectivity. Given the fine performances, the plasmonic biosensor is promising to be developed as a universal method for protein detection by choosing suitableaptamers, which may provide a platform for clinical diagnostics and pathogen detection for untrained personnel.

Acknowledgment

This work was financially supported by National Basic Research Program of China (No. 2011CB935704), the National Natural Science Foundation of China (No. 21235004, No. 21128005, No. 61405176).

References

Ahmad, A., Mukherjee, P., Mandal, D., Senapati, S., Khan, M.I., Kumar, R., Sastry, M., 2002. Enzyme mediated extracellular synthesis of CdS nanoparticles by the fungus. Fusarium oxysporum. J. Am. Chem. Soc. 124 (41), 12108–12109.
Boterashvili, M., Lahav, M., Shirman, T., Freeman, D., Van Der Boom, M.E., 2012. Integrated and Segregated Au/γ-Fe_2O_3 Binary Nanoparticle Assemblies. Angew. Chem. Int. Ed. 51 (49), 12268–12271.
Brown, K.R., Walter, D.G., Natan, M.J., 2000. Seeding of colloidal Au nanoparticle solutions. Improved control of particle size and shape. Chem. Mater. 12 (2), 306–313.
Chang, H., Tang, L., Wang, Y., Jiang, J., Li, J., 2010. Graphene fluorescence resonance energy transfer aptasensor for the thrombin detection. Anal. Chem. 82 (6), 2341–2346.
Chemla, Y.R., Crossman, H.L., Poon, Y., McDermott, R., Stevens, R., Alper, M.D., Clarke, J., 2000. Ultrasensitive magnetic biosensor for homogeneous immunoassay. Proc. Natl. Acad. Sci. U. S. A. 97 (26), 14268–14272.
Cho, H., Baker, B.R., Wachsmann-Hogiu, S., Pagba, C.V., Laurence, T.A., Lane, S.M., Lee, L.P., Tok, J.B.H., 2008. Aptamer-Based SERRS Sensor for Thrombin Detection. Nano Lett. 8 (12), 4386–4390.
de La Rica, R., Stevens, M.M., 2012. Plasmonic ELISA for the ultrasensitive detection of disease biomarkers with the naked eye. Nat. Nanotech. 7 (12), 821–824.
Deng, R.J., Tang, L.H., Tian, Q.Q., Wang, Y., Lin, L., Li, J.H., 2014. Toehold-initiated Rolling Circle Amplification for Visualizing Individual MicroRNAs in situ in Single Cells. Angew. Chem. Inter. Ed. 53 (9), 2389–2393.
Farokhzad, O.C., Cheng, J.J., Teply, B.A., Sherifi, I., Jon, S., Kantoff, P.W., Richie, J.P., Langer, R., 2006. Targeted nanoparticle-aptamer bioconjugates for cancer chemotherapy in vivo. Proc. Natl. Acad. Sci. U. S. A. 103 (16), 6315–6320.
Fredriksson, S., Gullberg, M., Jarvius, J., Olsson, C., Pietras, K., Gústafsdóttir, S.M., Östman, A., Landegren, U., 2002. Protein detection using proximity-dependent DNA ligation assays. Nat. Biotechnol. 20 (5), 473–477.
Goon, I.Y., Lai, L.M.H., Lim, M., Munroe, P., Gooding, J.J., Amal, R., 2009. Fabrication and Dispersion of Gold-Shell-Protected Magnetite Nanoparticles: Systematic Control Using Polyethyleneimine. Chem. Mater. 21 (4), 673–681.
Haes, A.J., Hall, W.P., Chang, L., Klein, W.L., Van Duyne, R.P., 2004. A localized surface plasmon resonance biosensor: First steps toward an assay for Alzheimer's disease. Nano Lett. 4 (6), 1029–1034.
Hao, D., Ohme-Takagi, M., Sarai, A., 1998. Unique mode of GCC box recognition by the DNA-binding domain of ethylene-responsive element-binding factor (ERF domain) in plant. J. Biol. Chem. 273 (41), 26857–26861.
He, P., Shen, L., Cao, Y., Li, D., 2007. Ultrasensitive electrochemical detection of proteins by amplification of aptamer-nanoparticle bio bar codes. Anal. Chem. 79 (21), 8024–8029.

Hui, C., Shen, C., Yang, T., Bao, L., Tian, J., Ding, H., Li, C., Gao, H.J., 2008. Large-scale Fe_3O_4 nanoparticles soluble in water synthesized by a facile method. J. Phys. Chem. C 112 (30), 11336–11339.
Huizenga, D.E., Szostak, J.W., 1995. A DNA aptamer that binds asenosine and ATP. Biochemistry 34 (2), 656–665.
Jana, N.R., Gearheart, L., Murphy, C.J., 2001. Seeding growth for size control of 5–40 nm diameter gold nanoparticles. Langmuir 17 (22), 6782–6786.
Jans, H., Huo, Q., 2012. Gold nanoparticle-enabled biological and chemical detection and analysis. Chem. Soc. Rev. 41 (7), 2849–2866.
Jiang, J., Gu, H., Shao, H., Devlin, E., Papaefthymiou, G.C., Ying, J.Y., 2008. Bifunctional Fe_3O_4-Ag Heterodimer Nanoparticles for Two-Photon Fluorescence Imaging and Magnetic Manipulation. Adv. Mater. 20 (23), 4403–4407.
Liu, D., Huang, X., Wang, Z., Jin, A., Sun, X.L., Zhu, L., Wang, F., Ma, Y., Niu, G., Hight Walker, A.R., 2013. Gold Nanoparticle-Based Activatable Probe for Sensing Ultralow Levels of Prostate-Specific Antigen. ACS Nano 7 (6), 5568–5576.
Liz-Marzan, L.M., 2006. Tailoring surface plasmons through the morphology and assembly of metal nanoparticles. Langmuir 22 (1), 32–41.
Luppa, P.B., Müller, C., Schlichtiger, A., Schlebusch, H., 2011. Point-of-care testing (POCT): Current techniques and future perspectives. TrAC Trends in. Anal. Chem. 30 (6), 887–898.
Macaya, R.F., Schultze, P., Smith, F.W., Roe, J.A., Feigon, J., 1993. Thrombin-bidning DNA aptamer forms a unimolecular quadruplex structure solution. Proc. Natl. Acad. Sci. U. S. A. 90 (8), 3745–3749.
Mayer, K.M., Hafner, J.H., 2011. Localized surface plasmon resonance sensors. Chem. Rev. 111 (6), 3828–3857.
McFarland, A.D., Van Duyne, R.P., 2003. Single silver nanoparticles as real-time optical sensors with zeptomole sensitivity. Nano Lett. 3 (8), 1057–1062.
Nie, H., Liu, S., Yu, R., Jiang, J., 2009. Phospholipid-Coated Carbon Nanotubes as Sensitive Electrochemical Labels with Controlled-Assembly-Mediated Signal Transduction for Magnetic Separation Immunoassay. Angew. Chem. Int. Ed. 48 (52), 9862–9866.
Pavlov, V., Xiao, Y., Shlyahovsky, B., Willner, I., 2004. Aptamer-functionalized Au nanoparticles for the amplified optical detection of thrombin. J. Am. Chem. Soc. 126 (38), 11768–11769.
Perez, J.M., Simeone, F.J., Saeki, Y., Josephson, L., Weissleder, R., 2003. Viral-induced self-assembly of magnetic nanoparticles allows the detection of viral particles in biological media. J. Am. Chem. Soc. 125 (34), 10192–10193.
Rangnekar, A., Sarma, T.K., Singh, A.K., Deka, J., Ramesh, A., Chattopadhyay, A., 2007. Retention of enzymatic activity of α-amylase in the reductive synthesis of gold nanoparticles. Langmuir 23 (10), 5700–5706.
Rodríguez-Lorenzo, L., de La Rica, R., Álvarez-Puebla, R.A., Liz-Marzán, L.M., Stevens, M.M., 2012. Plasmonic nanosensors with inverse sensitivity by means of enzyme-guided crystal growth. Nat. Mater. 11 (7), 604–607.
Rogstad, S.M., Sorkina, T., Sorkin, A., Wu, C.C., 2013. Improved Precision of Proteomic Measurements in Immunoprecipitation Based Purifications Using Relative Quantitation. Anal. Chem. 85 (9), 4301–4306.
Sepúlveda, B., Angelomé, P.C., Lechuga, L.M., Liz-Marzán, L.M., 2009. LSPR-based nanobiosensors. Nano Today 4 (3), 244–251.
Song, S., Qin, Y., He, Y., Huang, Q., Fan, C., Chen, H.-Y., 2010. Functional nanoprobes for ultrasensitive detection of biomolecules. Chem. Soc. Rev. 39 (11), 4234–4243.
Thompson, C.C., Brown, T.A., McKnight, S.L., 1991. Convergence of Ets-and notch-related structural motifs in a heteromeric DNA binding complex. Science 253 (5021), 762–768.
Tong, Y.K., Chiu, R.W.K., Chan, K.C.A., Leung, T.Y., Lo, Y.M.D., 2012. Technical concerns about immunoprecipitation of methylated fetal DNA for noninvasive trisomy 21 diagnosis. Nat. Med. 18 (9), 1327–1328.
Vallejo-Illarramendi, A., Marciano, D.K., Reichardt, L.F., 2013. A novel method that improves sensitivity of protein detection in PAGE and Western blot. Electrophoresis 34 (8), 1148–1150.
Wang, L.D., Tram, K., Ali Kha, M., Li, J.H., Li, Y.F., 2014. Arrest of Rolling Circle Amplification by Protein-Binding DNA Aptamers. Chem. J. Eur. 20 (9), 2420–2424.
Whitcombe, M.J., Chianella, I., Larcombe, L., Piletsky, S.A., Noble, J., Porter, R., Horgan, A., 2011. The rational development of molecularly imprinted polymer-based sensors for protein detection. Chem. Soc. Rev. 40 (3), 1547–1571.
Williams, T., Tjian, R., 1991. Characterization of a dimerization motif in AP-2 and its function in heterologous DNA-binding proteins. Science 251 (4997), 1067–1071.
Willner, I., Baron, R., Willner, B., 2006. Growing metal nanoparticles by enzymes. Adv. Mater. 18 (9), 1109–1120.
Zhang, X., Servos, M.R., Liu, J., 2012. Instantaneous and quantitative functionalization of gold nanoparticles with thiolated DNA using a pH-assisted and surfactant-free route. J. Am. Chem. Soc. 134 (17), 7266–7269.
Zhao, Y., Pan, H., Lou, Y., Qiu, X., Zhu, J., Burda, C., 2009. Plasmonic Cu_{2-x} S Nanocrystals: Optical and Structural Properties of Copper-Deficient Copper (I) Sulfides. J. Am. Chem. Soc. 131 (12), 4253–4261.